Wear and Frictional Behavior of Al 7075/FA/SiC Hybrid MMC's using Response Surface Methodology

Ravi Kumar Mandava (ravikumar1013@gmail.com)
Maulana Azad National Institute of Technology https://orcid.org/0000-0001-6186-9138
Vajram Venkata Reddy
Dire Dawa University
Veeravalli Rama Koteswara Rao
R.V.R & J.C College of Engineering

Research Article

Keywords: Al 7075, fly ash, silicon carbide, RSM, wear rate

Posted Date: February 15th, 2021

DOI: https://doi.org/10.21203/rs.3.rs-191669/v1

Version of Record: A version of this preprint was published at Silicon on August 16th, 2021. See the published version at https://doi.org/10.1007/s12633-021-01300-3.

Abstract

In the present research work an effort has been made to study the wear and frictional behavior of Aluminium Metal Matrix composite (Al 7075 as a base alloy and fly ash (FA) and silicon carbide (SiC) as reinforcements) by using the stir casting method. To carry out this work, the wt. % of reinforcements FA (2.5%, 5%, 7.5% and 10%) and SiC (2.5%, 5%, 7.5% and 10%)have been used 5%, 10%, 15% and 20%. Initially, the mechanical studies have been conducted and the best mechanical properties obtained at 20 wt. % of FA and SiC. Later on, the composite was fabricated by 20 wt. % of FA, SiC reinforcements are used to check the wear and frictional behavior on a pin-on-disc machine at the dry condition. The dry sliding wear behavior was carried out at various input parameters such as applied force (10N, 20N, and 30N), sliding velocity (1.5m/s, 3m/s, and 4.5m/s), and sliding distance (1000 m, 2000 m, and 3000 m). Further, a scanning electron microscope (SEM) are used to observe the mixing of reinforcements and examine the worn surfaces. A response surface methodology (RSM) is the reasonable and accurate method for conducting the experiments and identifying the optimal wear parameters. Moreover, the RSM was helped to identify the most significant factor, which was the influence on the wear rate. Finally, it is decided that the applying force is the utmost significant factor that leaves an effect on wear rate. The sliding velocity and distance are acting as the lesser influence on the performance indicator.

1. Introduction

In recent years, all aerospace, naval, and automobile industries are using aluminum metal matrix composites (AMMC's) due to their superior mechanical, tribological, and microstructural properties and lightweight. In general, AMMC's are modified based on the said application and numerous benefits, namely low coefficient of friction, adequate wear resistance, superior strength-to-weight-ratio, and elevated corrosion resistance. Therefore, wear is a significant parameter duly considered while design and manufacturing any machine elements and to ensure the performance is improved [1]. Through the particle dispersion, solid lubricant in the aluminum alloy can display better potential for wear resistance. Moreover, graphite is added in aluminum alloy because of better properties like low friction, chemical inertness, film-forming ability, and absence of inherent. The addition of graphite particulates with aluminum alloys can diminish the wear rate and also leads to a reduction in flexural strength and hardness [2]. To overcome the above problem, most of the researchers are adding both ceramics and lubricants for developing hybrid composites, which leads to achieving better mechanical and tribological properties [3–7]. Among other aluminum alloys, Al 7075 has owing the high strength and greater potential in dry sliding wear applications [8–9]. A numerous amount of research work [10–12] has been done to study the wear behavior of Al 7075 alloy reinforced with various ceramic reinforcements like silicon carbide (SiC), titanium carbide (TiC), alumina (Al_2O_3), graphite (Gr), titanium boride (TiB_2), etc. An investigation has been conducted on the effect of SiC and its particle size of Al 7075-SiC composites and observed that a significant enhancement in mechanical and tribological properties of the composite when to compare with base material [13]. Moreover, a study [14] has been carried out on the performance of wear on Al 7075 reinforced with Al_2O_3 composites and it has been fulfilled that the adding of ceramics improves the wear resistance. Further, an investigation [15] has been carried out on Al 7075 reinforced with B_4C

composites and observed that the enhancement in hardness and wear resistance but there is a reduction in COF. Baskaran et al. [16] discussed the wear behavior of Al 7075 reinforced with TiC and it can be observed that the behavior of wear reductions under dry conditions. Ranjan et al. [17] fabricated a composite using Al 7075 reinforced with TiB_2 particles and identified the tribological behavior on developed composites and they have mentioned higher wear resistance when increasing the TiB_2 particles. Recently, Idrisi et al. [18] fabricated a composite by Al6061 reinforced with SiC particles in various fractions using an ultrasonic vibration-based stir casting process. The author's observed after adding SiC particles the density, hardness, tensile, and compressive strength increase compared to the traditional stir casting process. In [19] the authors reported the hardness decreases with an increase in the graphite percentages with aluminum matrix. Moreover, Akhlaghi et al. [20] fabricated a composite by varying the Gr from 5–20% and Al2024 as a matrix. Once the experiments have been conducted the authors reported as the hardness and toughness of the composite have been reduced after adding the Gr as reinforcement. Further, Baradeswaranet al. [21] discussed after adding the Gr with Al 7075 the hardness was decreased, and the tensile strength was increased. In [22] Mohankumar et al. fabricated a composite with Al 359 as a matrix and B_4C and fly ash as the reinforcements using the stir casting technique. They discussed the hardness, tensile strength increases and the wear resistance also increases after adding fly ash and B_4C content. Dipankar et al. [23] fabricated a composite with the base metal Al 2024 and different weight percentages of SiC particulates and conduct the mechanical and tribological tests. The authors concluded that because of SiC particulates the mechanical and tribological properties are improved than the matrix alloy.

It is evident from the above literature, very few researchers had worked on the reinforcements of fly ash and SiC mixed with Al 7075. The mechanical and tribological properties of fly ash and SiC reinforcements are very minimal. Due to the formability, high strength to weight ratio, weldability, and corrosion resistance of Al 7075 alloy essentially using in structural, automobile, and aerospace applications. Therefore, the current research work is to develop the commercially based Al 7075 reinforced with SiC and fly ash powder based in situ composites using the stir casting technique. The reinforcements SiC and fly ash will enhance the mechanical and tribological properties. An RSM has been used for modeling the process parameters (that is, applying a load, sliding speed, and sliding distance) and planning the number of experiments. Further, mechanical properties like hardness, tensile strength, and tribological characteristics like wear rate, coefficient friction are studied in detail.

2. Materials And Methods

2.1 Materials and Instruments

The matrix Al 7075 and the reinforcement's fly ash, silicon carbide was procured from Venuka Engineering Private Limited, Hyderabad. The composites were prepared using a stir casting process, the mechanical properties such as hardness and tensile strength of the fabricated composites were measured on Vickers Hardness tester and tensometer. The tribological properties such as wear and coefficient of friction were measured on pin-on-disc apparatus and the scanning electron micrographs (SEM's) were taken from a

scanning electron microscope. Further, the chemical composition of the matrix Al 7075 alloy is given in Table 1.

Table 1.Chemical composition of AA 7075

Zn	Cu	Mg	Si	Cr	Mn	Fe	Pb	Sn	Ti	Al
5.6	1.3	2.4	0.4	0.18	0.3	0.5	0.03	0.012	0.2	89

2.2 Composite Fabrication

Al 7075 as a matrix and the reinforcements of 2.5%, 5%, 7.5%, and 10% of fly ash and silicon carbide prepared a composite using stir casting (ref. Fig. 1 (a)). Nearly 1000 grams of Al 7075 alloy small blocks are placed in a graphite crucible and melted up to the temperature of 850^0C. After reaching the 300^0C temperature a stirrer was introduced into the crucible for mixing the reinforcements uniformly. The weight percentages such as 2.5%, 5%, 7.5%, and 10% of fly ash and silicon carbide powder introduced into the crucible for preparation of composite. The stirrer was rotated at 500±10 rpm for 5 min and it was made by stainless steel sustained at 850^0C temperature. The stirring was continued until it to ensure proper mixing of reinforcements in a matrix. After completion of proper mixing, the liquid metal poured into a preheated mild steel moulds. Further, the composites (Fig.1 (b)) were kept into T_6 heat-treated conditions for conducting the hardness, tensile strength, and wear tests.

2.3 Density Test

Measurement of density (Fig.2) is one of the important properties to identify the porosity levels of the Al 7075 alloy and fabricated composite specimens. To determine the porosity level in the base alloy and fabricated composites, the experimental and theoretical densities were calculated. The Archimedes principle (Eq. (1)) is used to determine the experimental density values and the theoretical density values were determined by rules of mixtures (Eq. (2)).

$$\rho_{th} = \rho_m V_m + \rho_r V_r \quad (1)$$

$$\rho_{\exp} = \frac{Mass}{Volume} \quad (2)$$

2.4 Hardness and Tensile Test

Once the composites were prepared the specimens are cut into the hardness tests as per ASTM E10 standards. Moreover, determining the hardness values are a very important parameters for all fabricated composites. The conventional Vickers microhardness tester (Fig. 4(a)) with load 1 kg was used to measure the hardness values for both base and fabricated composite materials at room temperature. To avoid the indenter laying on the hard reinforcements the above test was conducted five various locations

on the specimens and the average value of all readings are reported. Further, the tensile specimens were machined into a cylindrical shape as per ASTM E8 standards is shown in Fig. 3. The prepared specimens were tested on a universal tensile testing machine (Fig. 4 (b)) with room temperature. For obtaining the accurate result three samples were tested in each category and the average value is reported.

2.5 Wear Test

To measure the wear properties on a pin-on-disk testing machine (Fig. 5) initially, the developed composite specimens were prepared with a diameter and height of 8 mm and 50 mm respectively. The counterface of the disc was prepared by EN 31 hardened steel with a thickness and diameter of 5 mm and 90 mm respectively. Before conducting the experiment, both sides of the specimens were polished by using different sizes of emery papers. Further, the wear test was conducted by changing the sliding speed of 1.5 - 4.5m/s, the sliding distance of 1000 – 3000m, and applying a load of 10-30 N under atmospheric room temperature. While conducting the experiment before and after each test the weight of the specimens was measured using a weighing machine with a precision of 0.001 mg. The wear rate was calculated using the difference between the volumetric loss per unit sliding distance earlier and later of each test. Moreover, normal force, friction force, and sliding surfaces of contact were recorded by a load cell continuously for measuring the COF. The morphologies of the worn surfaces of the tested samples were examined using SEM.

2.6 Response Surface Methodology (RSM)

RSM adopts both mathematical and statistical techniques, which are helpful to determine the both modeling and analysis of the problems. Moreover, this method will also help to estimating the coefficients, studying the responses based on the combinations, fitting with the experimental data, predicting the response, and checking the adequacy of the fitted model [24]. The sliding speed, sliding distance, and applying load are selected as independent variables and the wear rate and coefficient friction are treated as response variables. The initial input variables are, sliding speed was varied between the two levels 1.5 and 4.5 m/s relatives to the center point 3 m/s. The second input variable that is, the sliding distance was varied between the two levels 1000 and 3000 m relative center point 2000 m. Further, the third input variable that is, applying load was varied between the 10 and 30 N with the center point 20 N. Alongside, the wear rate, and COF are the dependent variables.

3. Results And Discussion

The matrix of aluminum 7075 and reinforcements SiC and fly ash composites are fabricated using the stir casting technique. The fabricated composites are used to investigate the density, micro-hardness, tensile strength, % of elongation, wear and frictional behavior and examine the analysis of the microstructure.

3.1 Density

The experimental and theoretical densities of the composite material are shown in Fig. 6. It can be observed that the density of the fabricated composite (after adding the reinforcements such as, fly ash and SiC) was low compared to the base material. Moreover, it can also be observed that the density decreases when the percentage of reinforcements increases. Similar trends were also observed the previous researchers [24–26]. Further, the density of the experimental was low compared to the theoretical density. It may be due to the porosity increases while fabricating the composite.

3.2 Microhardness

The surface of the fabricated hybrid composite samples and base material has been prepared to determine the hardness value. Figure 7 shows the Vickers microhardness values for both base and composites. It can be observed that the hardness of the fabricated composite specimens was increased compared to the base aluminum 7075 alloys. Moreover, it is clearly understood that the hardness of the fabricated composite was increased while increasing the weight percentage of SiC and fly ash reinforcements. The hardness of the base material to composites increases from 102 VHN to 127 VHN. It may be due to the reason, fly ash particulates consists high in silica and alumina which are hard. Due to the better strain energy, the hardness of the developed composites is increased at the peripheral of the particles dispersed in the matrix. Therefore, the uniform dispersion of reinforcements causes the enhancement of hardness and rigidity of the composite.

3.3 Tensile strength

Figure 8 shows the variation of tensile strength, yield strength, and young's modulus with varying SiC and fly ash. The tensile strength, yield strength, and young's modulus increase with increasing the SiC and fly ash content and it is significantly greater than the strength of the base alloy. It may due to the reason SiC and fly ash reinforcements exhibits a perfect bonding with Al 7075 alloy which helps in enduring more loads as compared to Al 7075 alloy. The structure and properties of SiC and fly ash particles builds a strong interface between matrix to reinforcements and showing the better tensile strength.

3.4 Dry sliding wear behavior

After conducting the mechanical tests the hardness and tensile of the developed hybrid composites were achieved the best results at 10% reinforcements of SiC and fly ash. Further, the dry sliding wear behavior was conducted at 10% of SiC and fly ash hybrid composites. A statistical method in Minitab (Response Surface Methodology) was used to design the experiment, developing the models, and analyzing the results. A central composite design was selected for conducting the experiments. Table 2 shows the input parameters with their levels used for the current study. Based on the number of input variables and levels (shown in Table 2) the number of experiments was planned for the present study is given in Table 3. The significance values of the coefficients were tested at a 95% confidence level using the MINITAB 16. Later on, the developed mathematical models were established to estimate the wear rate and COF. The mathematical expressions for the hybrid composites are given below.

Wear rate (WR) = -0.205 + 0.2309*Sliding speed + 0.000048*Sliding distance + 0.0465 *Applying load − 0.0511*Sliding speed* Sliding speed − 0.000589*Applying load* Applying load + 0.000022* Sliding speed

*Sliding distance − 0.000766 * Sliding speed * Applying load − 0.000008 *Sliding distance * Applying load

Coefficient of friction (CoF) = 1.880 + 0.0575*Sliding speed- 0.000022*Sliding distance- 0.1209*Applying Load − 0.0421*Sliding speed *Sliding speed + 0.002157 *Applying Load *Applying Load + 0.000030*Sliding speed*Sliding distance + 0.00283 *Sliding speed*Applying Load + 0.000005 *Sliding distance * Applying Load

Table 2
Input levels of wear parameters

S.No	Parameters	Levels		
		Low (-1)	Medium (0)	High (+ 1)
1	Applying load (N)	10	20	30
2	Sliding speed (m/s)	1.5	3	4.5
3	Sliding distance (m)	1000	2000	3000

Table 3
Design matrix and wear result

Std Order	Run Order	Sliding Speed (m/s)	Sliding Distance (m)	Applying Load (N)	Wear Rate (mm^3/m)	Coefficient of Friction
1	19	1.5	1000	10	0.360275	0.950
2	2	4.5	1000	10	0.244166	0.490
3	13	1.5	3000	10	0.189907	0.625
4	6	4.5	3000	10	0.126605	0.475
5	14	1.5	1000	30	0.678240	0.410
6	17	4.5	1000	30	0.434074	0.250
7	11	1.5	3000	30	0.094227	0.410
8	4	4.5	3000	30	0.067098	0.300
9	7	1.5	2000	20	0.501898	0.480
10	8	4.5	2000	20	0.257731	0.180
11	5	3.0	1000	20	0.596851	0.400
12	12	3.0	3000	20	0.343642	0.350
13	15	3.0	2000	10	0.406944	0.875
14	20	3.0	2000	30	0.464998	0.406
15	16	3.0	2000	20	0.458000	0.426
16	1	3.0	2000	20	0.484000	0.419
17	18	3.0	2000	20	0.495998	0.405
18	3	3.0	2000	20	0.435500	0.421
19	9	3.0	2000	20	0.444998	0.405
20	10	3.0	2000	20	0.475500	0.416

Testing the data and competence of the model

The normal probability graph of the residuals for wear rate and COF of the fabricated hybrid composites has shown in Fig. 9. It has been observed that the residuals are falling on the straight line and the means of errors were distributed normally. Moreover, it can also confirm that there was no predictable pattern observed because all the run residues lay on or between the levels. The ANOVA technique was used to test the significance of the established model and the coefficient specifies the goodness of fits of the model. The ANOVA results related to the wear rate and COF for their levels, factors, and their interactions are given

in Tables 4 and 5. In the present problem, the value of the coefficient for wear rate (R^2 = 0.9666) and coefficient of friction (R^2 = 0.9610) indicates that only less than 5% of the total variance. Further, the adjusted coefficient for wear rate (adjusted R^2 = 0.9365) and coefficient of friction (adjusted R^2 = 0.9259) is also high, which means the significance of the model is high. Based on the above results it can be observed that the predicted R^2 value is also better than the adjusted R^2. The ANOVA result of wear rate and coefficient of friction for the developed hybrid composites is shown in Tables 4 and 5 which indicates that the predictability of the developed model for wear rate and coefficient of friction is at a 95% confidence level because the value of p is less than the 0.05 in most of the cases even though the value of p is more than the 0.05 such parameters are not that much influence on the significant level.

Table 4. Variance for Wear rate

Source	DF	Adj SS	Adj MS	F-Value	P-Value
Model	9	0.505943	0.056216	32.13	0.000
Linear	3	0.287800	0.095933	54.83	0.000
Speed	1	0.048285	0.048285	27.60	0.000
SD	1	0.222645	0.222645	127.26	0.000
Load	1	0.016871	0.016871	9.64	0.011
Square	3	0.153029	0.051010	29.16	0.000
Speed*Speed	1	0.036419	0.036419	20.82	0.001
SD*SD	1	0.001671	0.001671	0.95	0.352
Load*Load	1	0.009548	0.009548	5.46	0.042
2-Way Interaction	3	0.065113	0.021704	12.41	0.001
Speed*SD	1	0.009102	0.009102	5.20	0.046
Speed*Load	1	0.001055	0.001055	0.60	0.455
SD*Load	1	0.054956	0.054956	31.41	0.000
Error	10	0.017496	0.001750		
Lack-of-Fit	5	0.014747	0.002949	5.36	0.044
Pure Error	5	0.002749	0.000550		
Total	19	0.523439			

Table 5: Variance for Coefficient of friction

Source	DF	Adj SS	Adj MS	F-Value	P-Value
Model	9	0.600219	0.066691	27.40	0.000
Linear	3	0.419432	0.139811	57.43	0.000
Speed	1	0.139240	0.139240	57.20	0.000
SD	1	0.011560	0.011560	4.75	0.054
Load	1	0.268632	0.268632	110.35	0.000
Square	3	0.131124	0.043708	17.95	0.000
Speed*Speed	1	0.024724	0.024724	10.16	0.010
SD*SD	1	0.006825	0.006825	2.80	0.125
Load*Load	1	0.127926	0.127926	52.55	0.000
2-Way Interaction	3	0.049662	0.016554	6.80	0.009
Speed*SD	1	0.016200	0.016200	6.65	0.027
Speed*Load	1	0.014450	0.014450	5.94	0.035
SD*Load	1	0.019012	0.019012	7.81	0.019
Error	10	0.024344	0.002434		
Lack-of-Fit	5	0.023970	0.004794	64.21	0.000
Pure Error	5	0.000373	0.000075		
Total	19	0.624563			

Figures 10 (a), (b), and (c) show the 3D surface and 2D contour plots of the wear rate were plotted from table 3, to identify the responses of various combinations of independent variables. Figure 10(a) shows initially, the wear rate is high with increasing the applying load and the sliding distance was small. Later on, the wear rate decreases with increasing the sliding distance and applying load. It may be due to the reason at initial due to more applying load the specimen more contact with the disc and it will wear more. Moreover, figure 10(b) shows the wear rate was small at initial and slowly wear rate increases when the sliding speed and applying load increases but, at the end of the sliding speed the wear rate was small. Further, figure 10(c) shows the wear rate increases when the sliding distance and sliding speed was small and slowly decreases when the sliding speed increases. It was observed that the applying load had the most dominant effect on wear rate concerning sliding distance and sliding speed.

Figure 11 (a), (b), and (c) show the 3D surface and 2D contour plots of the COF concerning three input variables such as sliding distance, applying load, and sliding speed. From figure 11(a) it has been observed that the COF is high when the sliding distance is small and the applying load is small. Similarly, from figure 11(b) it has been observed that the COF is low when the sliding speed is high concerning applying load. It can be observed that the presence of blue regions shows in the contour plot has the minimum COF. Finally, figure 11 (c) shows that, it has been observed that the COF is high when sliding speed low but, COF decreases slowly when increasing the sliding speed and distance.

Figure 12 shows the SEM worn surface morphology of the selected specimen with the reinforcement of 10% FA and 10% after SiC. It can be noted that the analysis of worn surfaces indicates that the delamination, abrasion, and adhesion mechanisms are leading in this alloy. Further, the delamination, abrasion, and oxidation on wear mechanisms were recognized and examined. Severe surface wear,

delamination, peeling of the matrix, grooves, plowing, scratches were recognized in the composite. Moreover, the aluminum alloy contacts with the EN31 steel disk to form an adhesive layer at the contacting asperities. It may be happened due to the high frictional temperature produced during sliding contact at the interface. Also, in the case of the base alloy, the appearance of shear-like crack characteristics on worn surfaces as represented by arrows reveals that the dominance wear mechanism is delaminated.

3.5 Confirmation tests

The wear behavior of Al 7075+10%FA+10% SiC hybrid composite was conducted with various input parameters using a central composite design (Table 3). The confirmatory experimentations have been accompanied to check the precision of the established model and results are displayed in Table 6. Further, the acquired investigational results were well correlated with the predicted results by the developed model. Moreover, it can be observed that the obtained all confirmatory results were produced an error value is less than 5% which specifies more reliability. Based on the above results it can be ensured that the developed model was generating good and accurate results. Hence, the developed hybrid composite has been generated superior wear-resistant properties in the long run which can be suitable for automobile, aerospace, and marine applications.

Table. 6 Conformation results for the developed model.

S.NO	Sliding Speed (m/s)	Sliding Distance (m)	Applying Load (N)	Experimental		Regression		% of error in WR	% of error in a COF
				WR (mm^3/m)	COF	WR (mm^3/m)	COF		
1	2.0	1400	14	0.5562	0.8017	0.5385	0.7872	3.29	1.84
2	2.5	1800	18	0.6026	0.6954	0.5907	0.6680	2.01	4.10
3	3.5	2200	22	0.5634	0.6124	0.5439	0.5922	3.58	3.41
4	4.0	2600	26	0.4658	0.6499	0.4449	0.6382	4.69	1.83

4. Conclusions

Based on the above experimental work, the subsequent conclusions are made as follows:

- The matrix Al 7075 and reinforcements FA and SiC with different weight percentages vary from 0%, 2.5%, 5%, 7.5%, and 10% were effectively fabricated using the stir casting technic and therefore the mechanical behavior was evaluated.
- Better mechanical properties were achieved at Al 7075 with 10% FA and 10% SiC and the said specimens were used to estimate the wear rate.
- RSM was used to estimate the wear rate at various settings such as applying a load, sliding distance, and sliding speed, and the optimal wear rate was also attained.

- Moreover, the developed statistical ANOVA effects were revealed that the applying load was contributed to a high wear rate concerning sliding distance and sliding speed.
- Further, the morphology study has been studied for optimal wear rate specimen and identifying the plowing, asperities, adhesion, and sliding direction.
- Finally, Al 7075 with 10% FA and SiC hybrid composite has been evidenced to be an efficient material that is useful in aerospace, automobile, and marine applications.

Declarations

Ethics approval and consent to participate

The authors following the ethics while preparing the material and writing the article.

Consent for publication

Yes. The authors are agreed to publish the work after accepting.

Availability of data and materials

Yes. If any data is required realted to this article the authors are ready to provide.

Competing interests

Not Applicable.

Funding

Not Applicable.

Authors' contributions

First author: He is actively involved in preparation of composites, analysing the results and writing the article.

Second Author: He is highly involved in testing the mechanical properties and tribological properties.

Third Author: He is actively involved in Prepartion of the composites, testing the materials and writing the article.

Acknowledgements

Not applicable.

References

1. Deuis RL, Subramanian C, Yellup JM. Dry sliding wear of aluminum composites – a review. Compos SciTechnol 1997;57:415–35.
2. Jun D, Yao-hui L, Si-rong Y, Wen-fang L. Dry sliding friction and wear properties of Al2O3 and carbon short fibers reinforced Al–12Si alloy hybrid composites. Wear 2004;257:930–40.
3. Vettivel SC, Selvakumar N, Vijay Ponraj P. Mechanical behavior of sintered Cu-5% W nanocomposite. ProcedEng 2012;38:2874–80.
4. Zhan Y, Zhang G. The role of graphite particles in the high-temperature wear of copper hybrid composites against steel. Mater Des 2006;27:79–84.
5. Rao RN, Das S. Effect of matrix alloy and influence of SiC particle on the sliding wear characteristics of aluminium alloy composites. Mater Des 2010;31:1200–7.
6. Rao RN, Das S, Mondal DP, Dixit G. Dry sliding wear behavior of cast high strength aluminium alloy (Al–Zn–Mg) and hard particle composites. Wear 2009;267:1688–95.
7. Toptan F, Kilicarslan A, Karaaslan A, Cigdem M, Kerti I. Processing and microstructural characterization of AA 1070 and AA 6063 matrix B4Cp reinforced composites. Mater Des 2010; 31:87–91.
8. Bai Y, Guo Y, Li J, Yang Z, Tian J (2017) Effect of Al2O3 nanoparticle reinforcement on the mechanical and high-temperature tribological behavior of Al-7075 alloy. ProcInstMechEng Part J JEngTribol 231:900–909.
9. Ebrahimzad P, Ghasempar M, Balali M (2017) Friction stir processing of aerospace aluminum alloy by addition of carbon nanotube. Trans Indian Inst Met 70:2241–2253.
10. Shanmughasundaram P (2015) Statistical analysis on the influence of heat treatment, load, and velocity on the dry sliding wear behavior of aluminum alloy 7075. Mater PhysMech 118–124.
11. Ruiz-Andres M, Conde A, De Damborenea J, Garcia I (2015) ´ Wear behavior of aluminum alloys at slow sliding speeds. Tribol Trans 58:955–962.
12. Yang Z-R, Sun Y, Li X-X, Wang S-Q, Mao T-J (2015) Dry sliding wear performance of 7075 Al alloy under different temperatures and load conditions. Rare Met 1–6. https://doi.org/10.1007/ s12598-015-0504-7.
13. Rao TB (2017) An experimental investigation on mechanical and wear properties of Al 7075/SiCp composites: effect of SiC content and particle size. J Tribol 140:31601–31608.
14. Baradeswaran A, Elayaperumal A, Franklin Issac R (2013) A statistical analysis of optimization of wear behavior of Al- Al 2O3 composites using Taguchi technique. preceding 64(Elsevier):973–982.
15. Baradeswaran A, ElayaPerumal A (2013) Influence of B4C on the tribological and mechanical properties of Al 7075-B4C composites. Compos Part B Eng 54:146–1152.
16. Baskaran S, Anandakrishnan V, Duraiselvam M (2014) Investigations on dry sliding wear behavior of in situ casted AA7075-TiC metal matrix composites by using Taguchi technique. Mater Des 60:184–192.
17. Michael Rajan HB, Ramabalan S, Dinaharan I, Vijay SJ (2014) Effect of TiB2 content and temperature on sliding wear behavior of AA7075/TiB2 in situ aluminum cast composites. Arch CivMechEng

14:72–79.
18. Idrisi AH, Mourad A-HI (2019) Conventional stir casting versus ultrasonic-assisted stir casting process: mechanical and physical characteristics of AMCs. J Alloys Compd 805:502.
19. Hassan AM, Tashtoush GM, Al-Khalil JA (2007) Effect of graphite and/or silicon carbide particles addition on the hardness and surface roughness of Al-4 wt% Mg alloy. J Compos Mater 41:453–465.
20. Akhlaghi F, Zare-Bidaki A (2009) Influence of graphite content on the dry sliding and oil-impregnated sliding wear behavior of Al 2024—graphite composites produced by in situ powder metallurgy method. Wear 266:37–45.
21. Baradeswaran A, Perumal AE (2014) Wear and mechanical characteristics of Al 7075/graphite composites. Composites B 56:472–476.
22. Mohankumar S, Aravind RA, SelvaKumar G, Raja P, Selvam V, (2020) Experimental investigation on the tribological -mechanical properties of B4C and fly ash reinforced Al 359 composites. Materials Today: Proceedings 21: 748-754.
23. Dipankar Dey & Abhijit Bhowmik & Ajay Biswas (2020) Effect of SiC Content on Mechanical and Tribological Properties of Al2024-SiC Composites. Silicon, https://doi.org/10.1007/s12633-020-00757-y.
24. Vettivel SC, Selvakumar N, Narayanasamy R, Leema N. Numerical modeling, prediction of Cu–W nanopowder composite in dry sliding wear condition using response surface methodology. Mater Des 2013;50:977–96.

Figures

Figure 1

Schematic diagram showing the (a) stir casting process and (b) casted specimens.

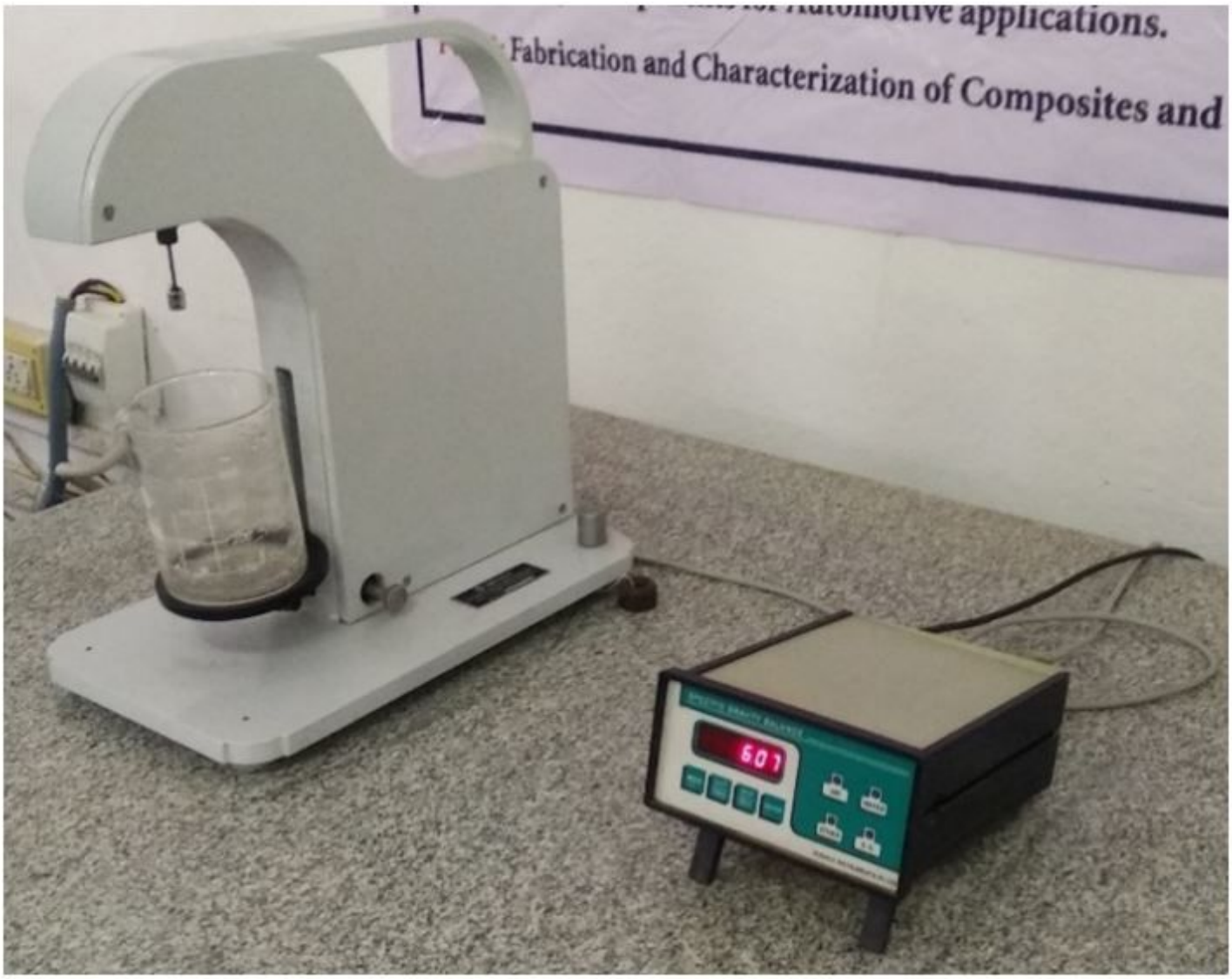

Figure 2

Density tester.

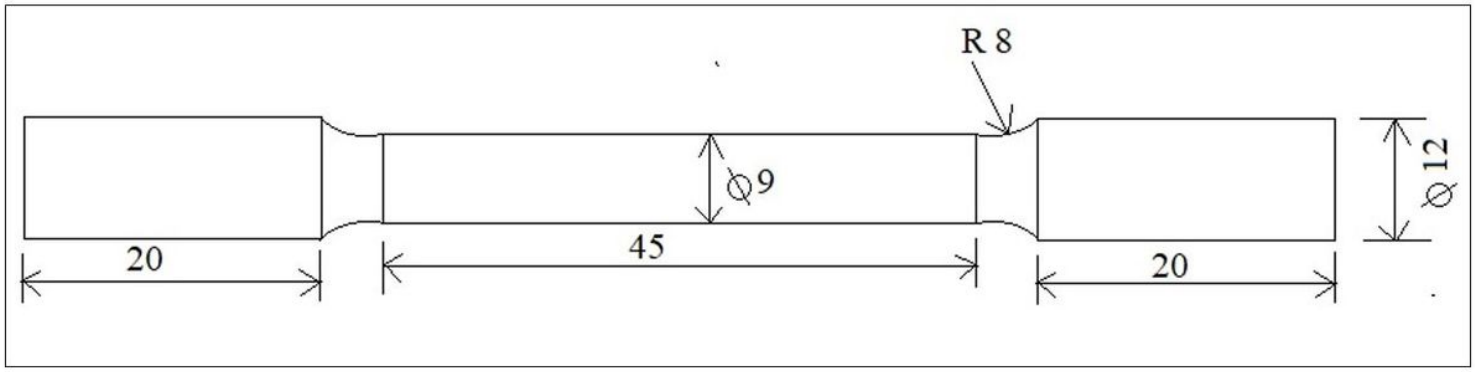

Figure 3

Dimensions of the tensile specimens as per ASTM E8 standards.

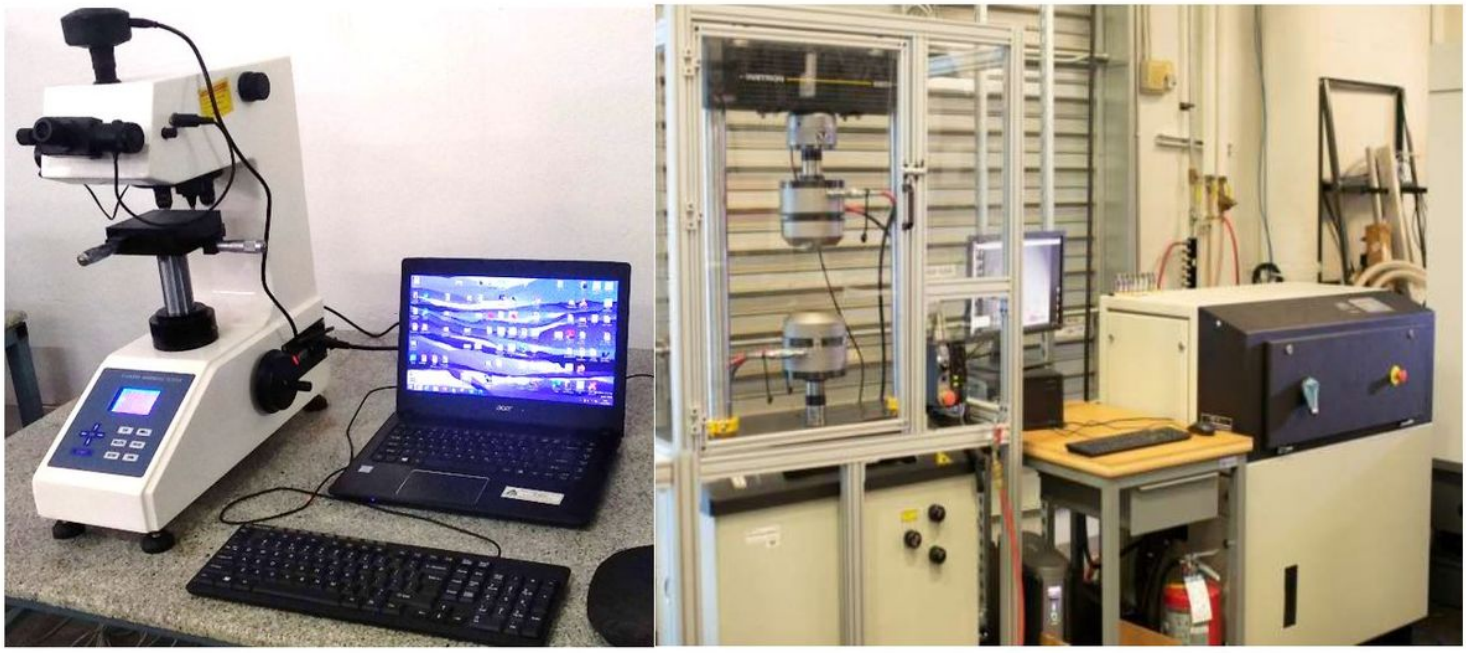

(a) (b)

Figure 4

Schematic diagram showing the (a) Vickers microhardness tester and (b) tensile tester.

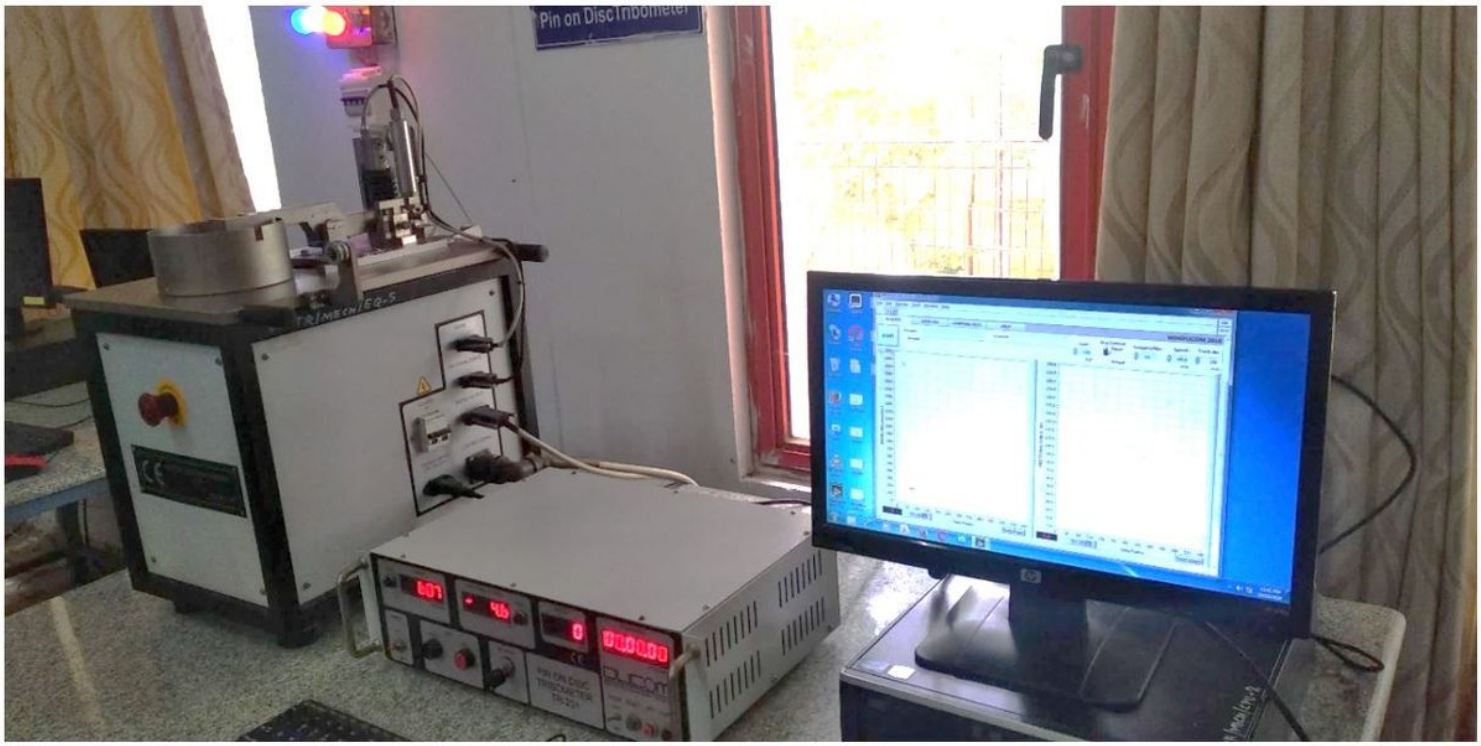

Figure 5

Pin-on-disc apparatus.

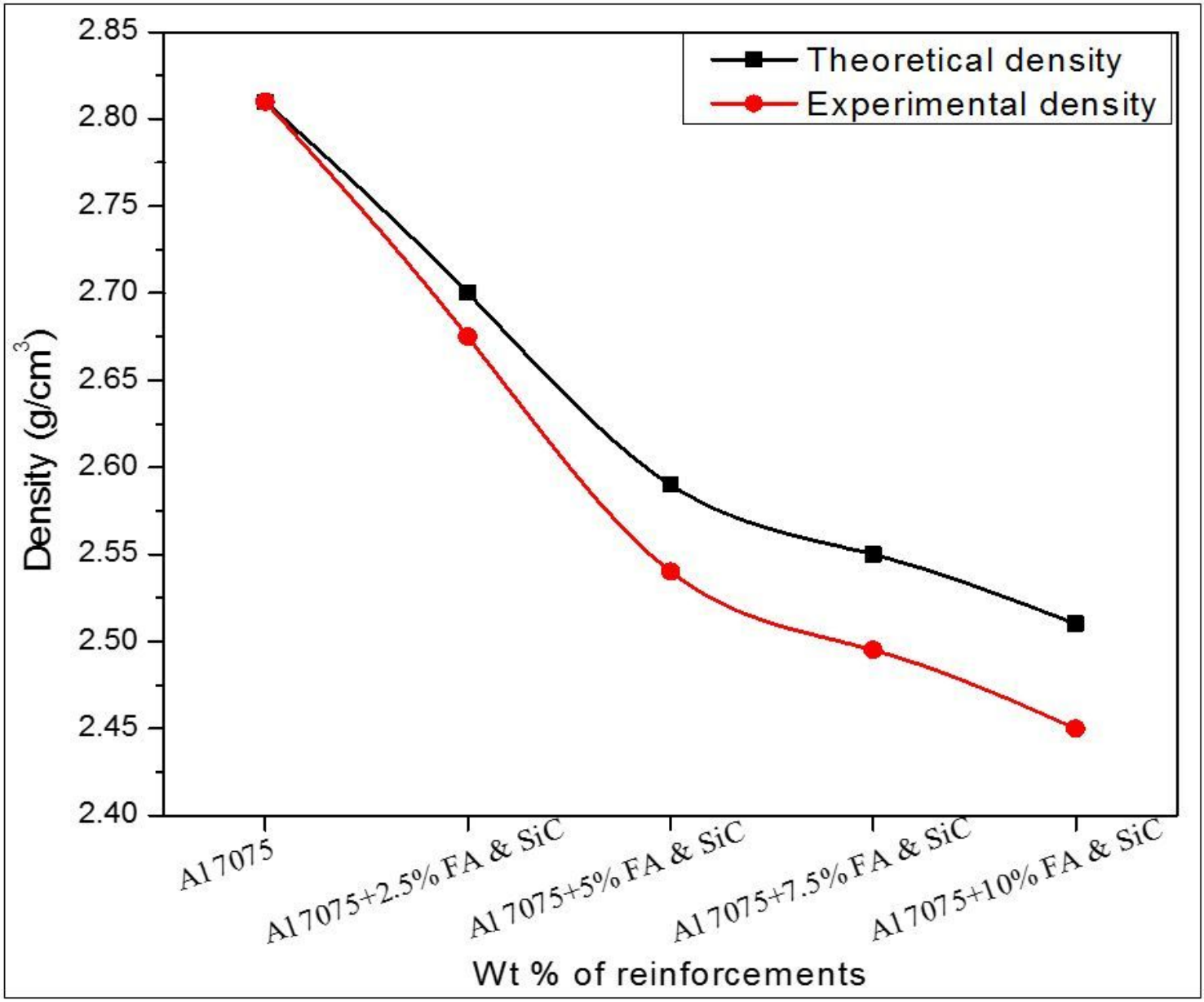

Figure 6

Variation of density with wt. % of reinforcements.

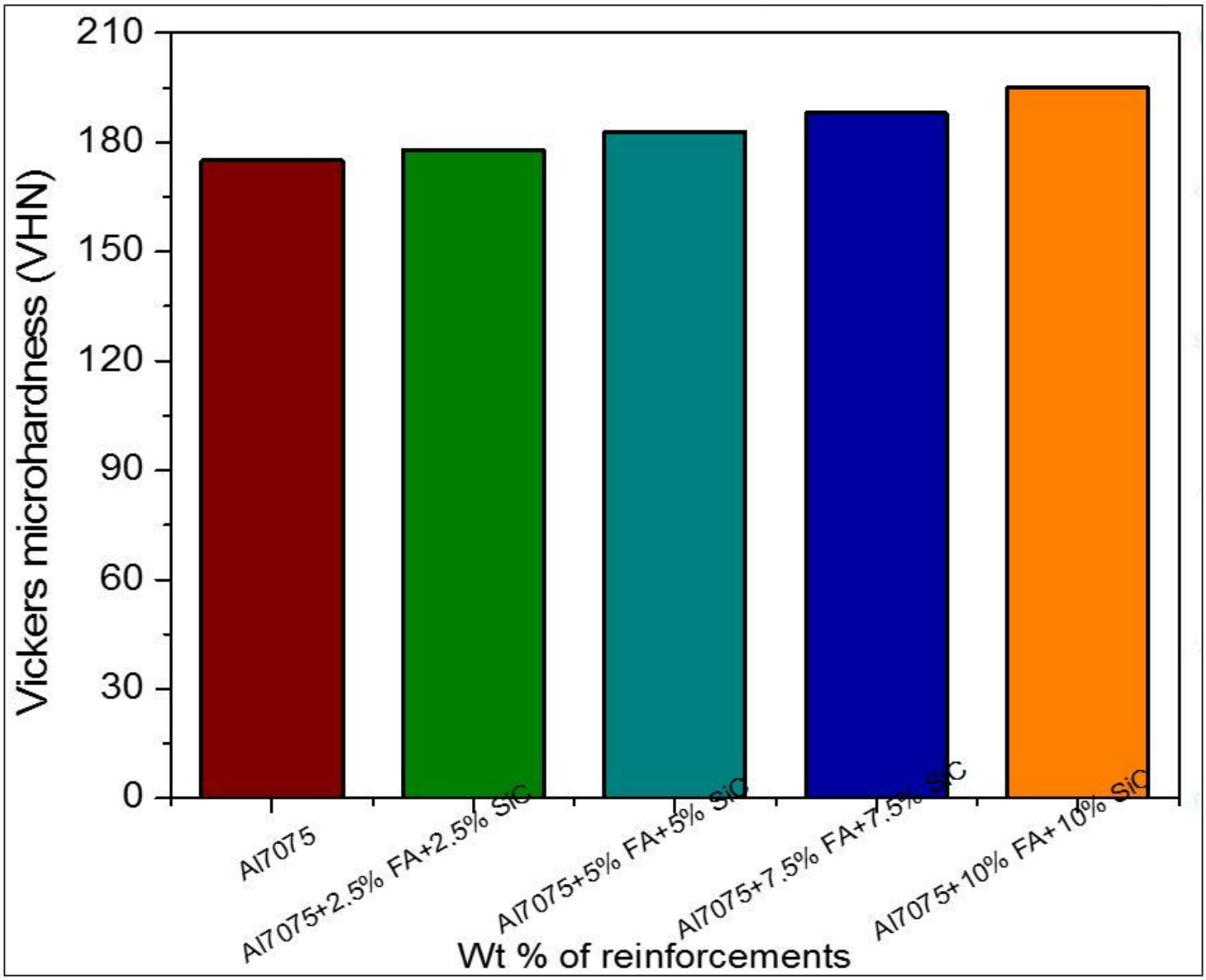

Figure 7

Variation of Vickers microhardness with wt % of reinforcements.

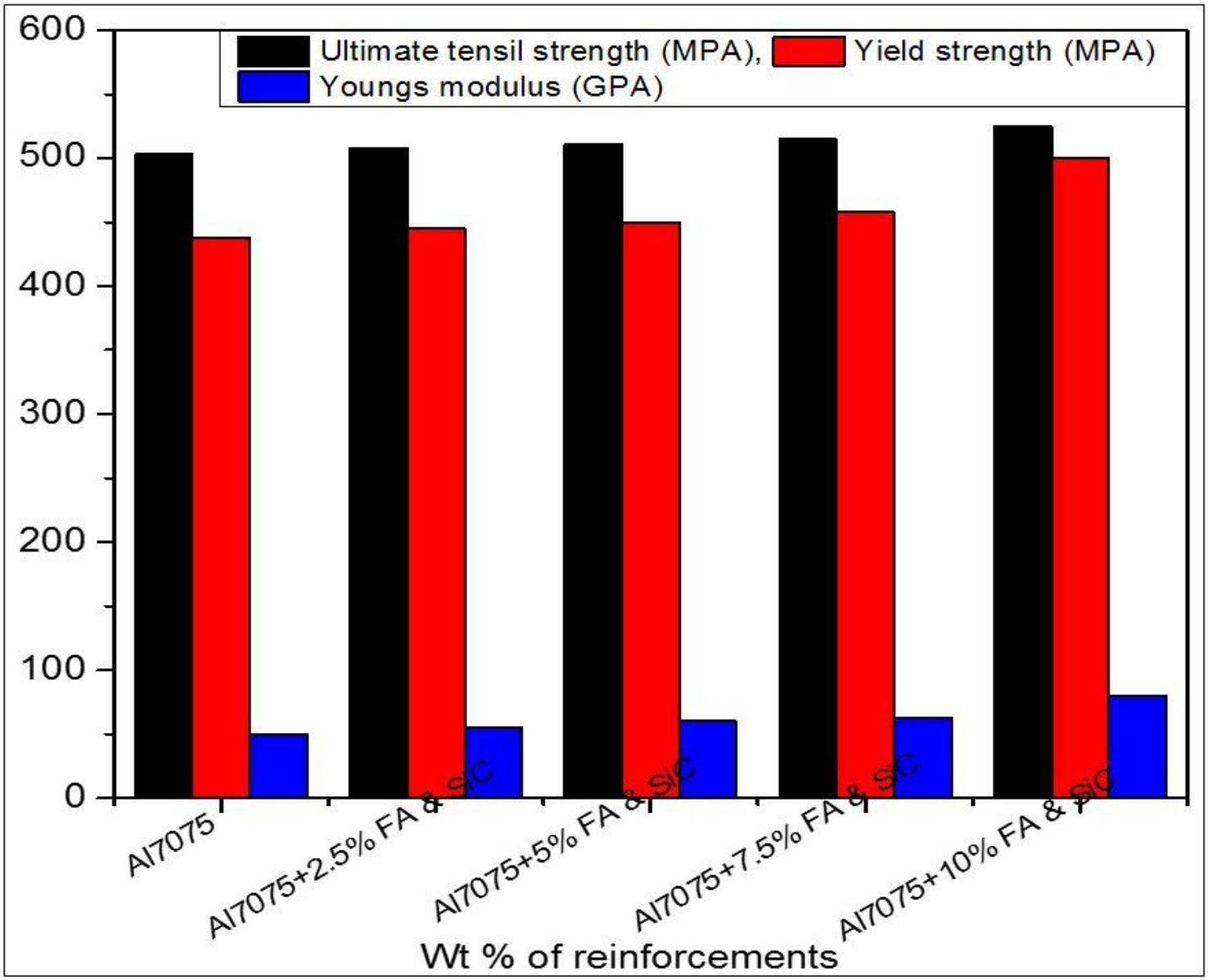

Figure 8

Variation of tensile strength, yield strength, and young's modulus with wt % of reinforcements.

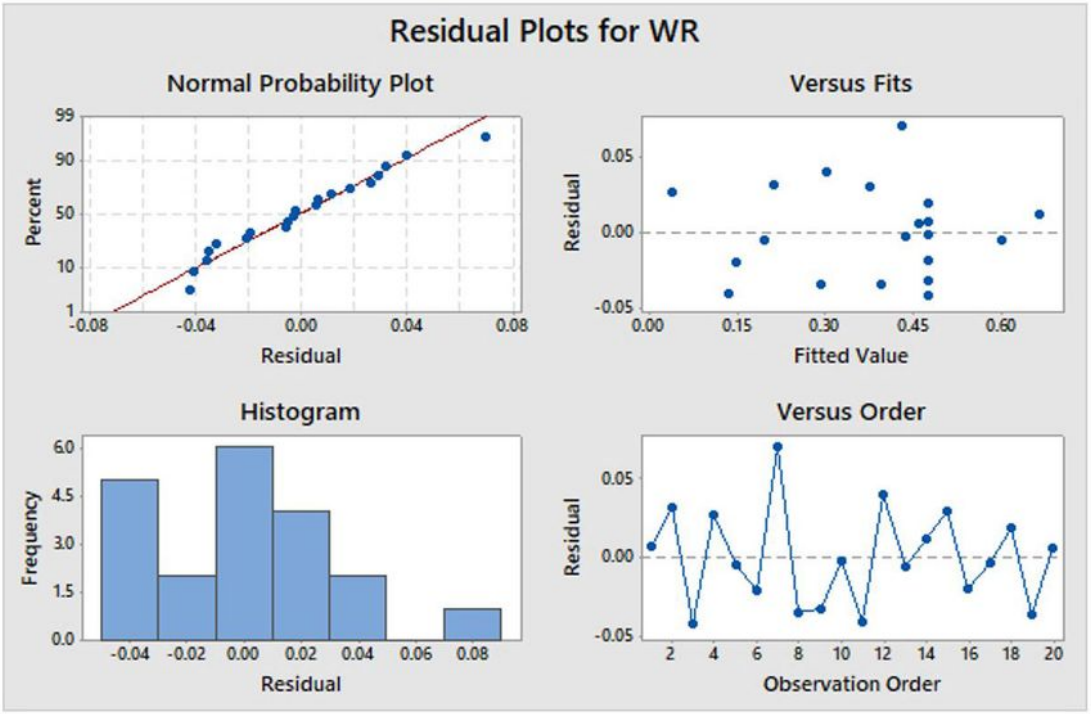

(a)

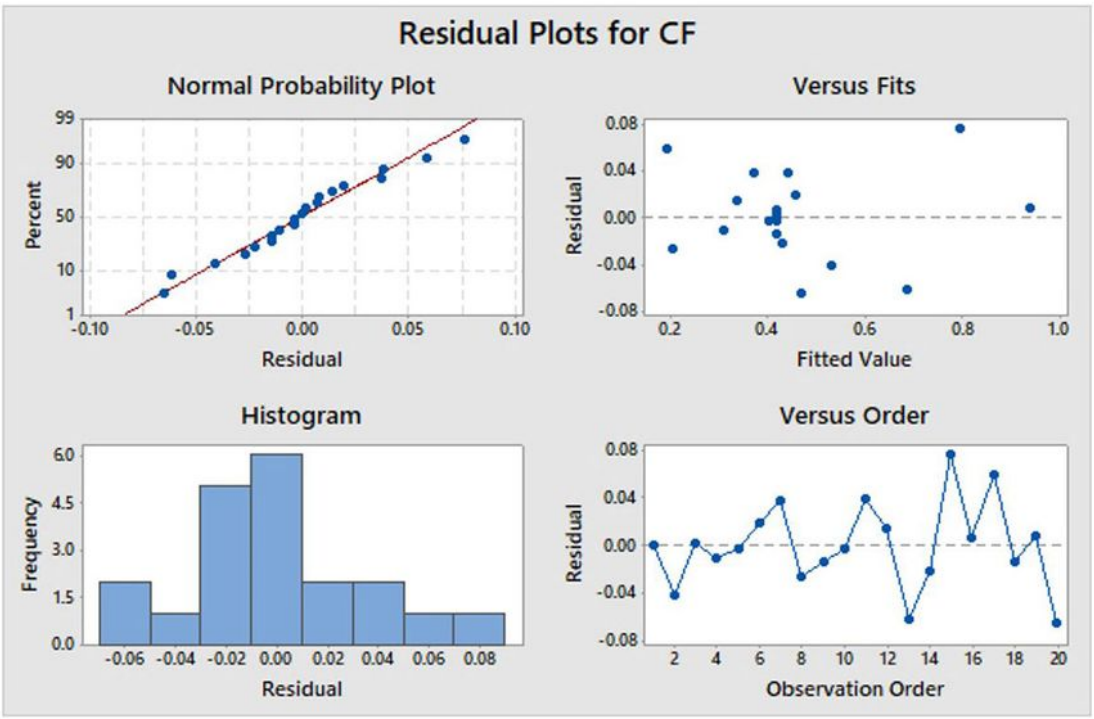

(b)

Figure 9

Residual plots (a) wear rate, and (b) coefficient of friction.

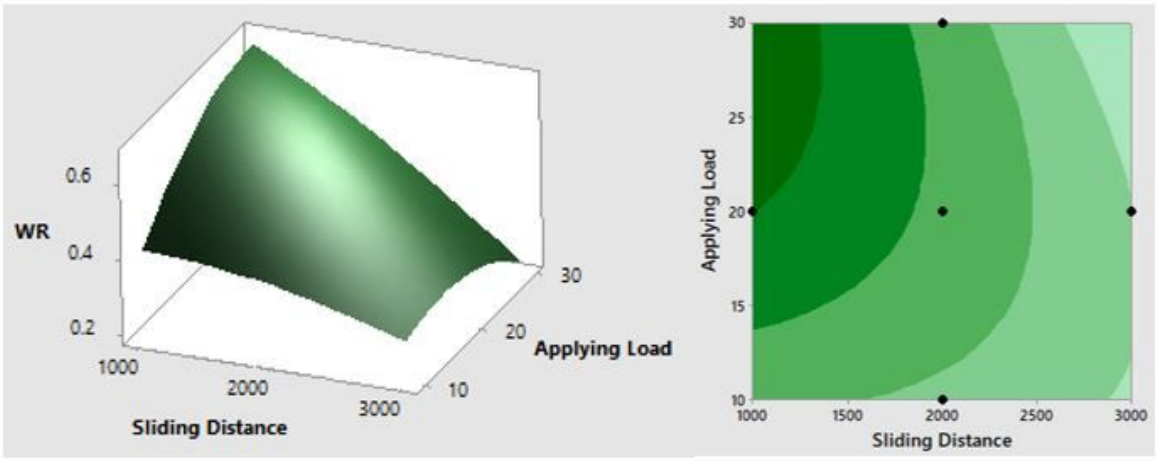

Figure 10

3D surface and contour plots for predicting the wear rate (a) sliding distance vs applying a load, (b) sliding speed vs applying load, and (c) sliding speed vs sliding distance.

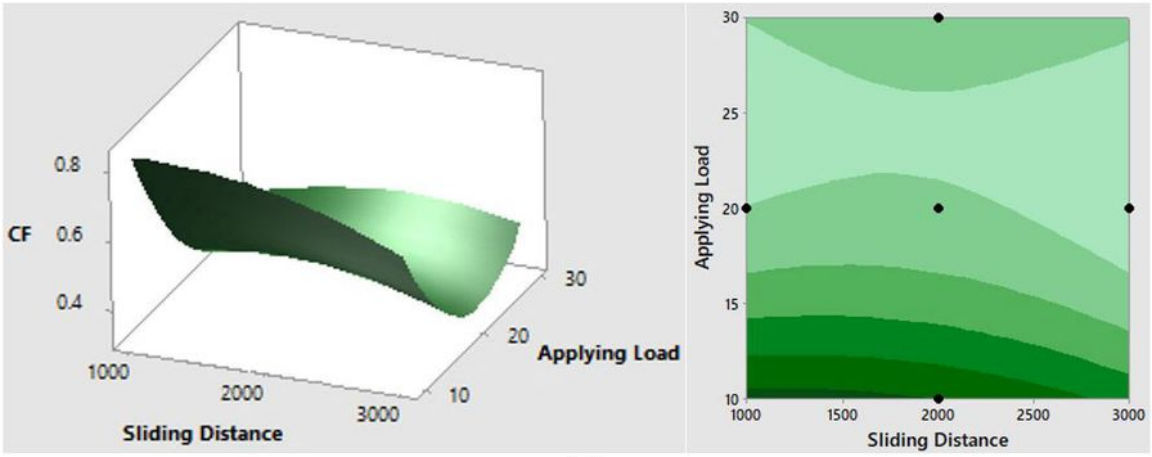

(a)

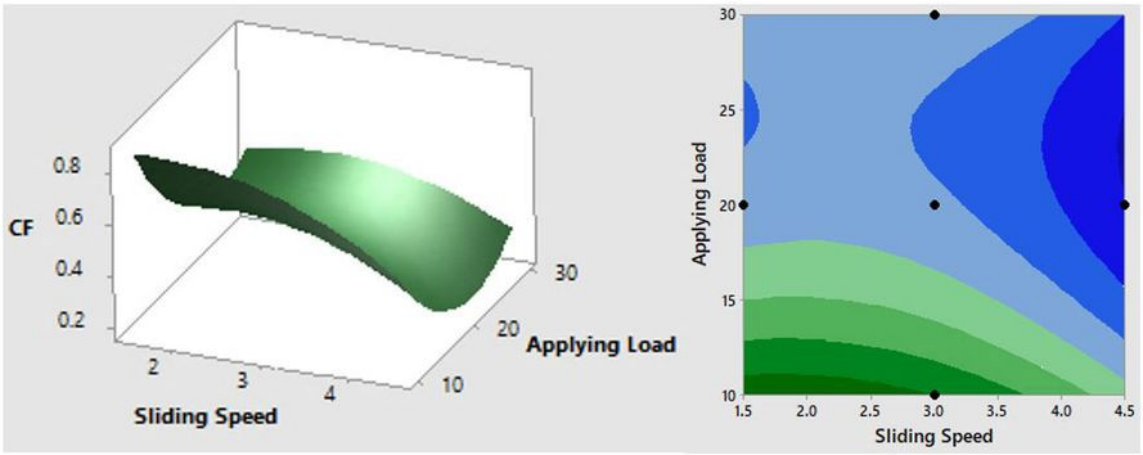

(b)

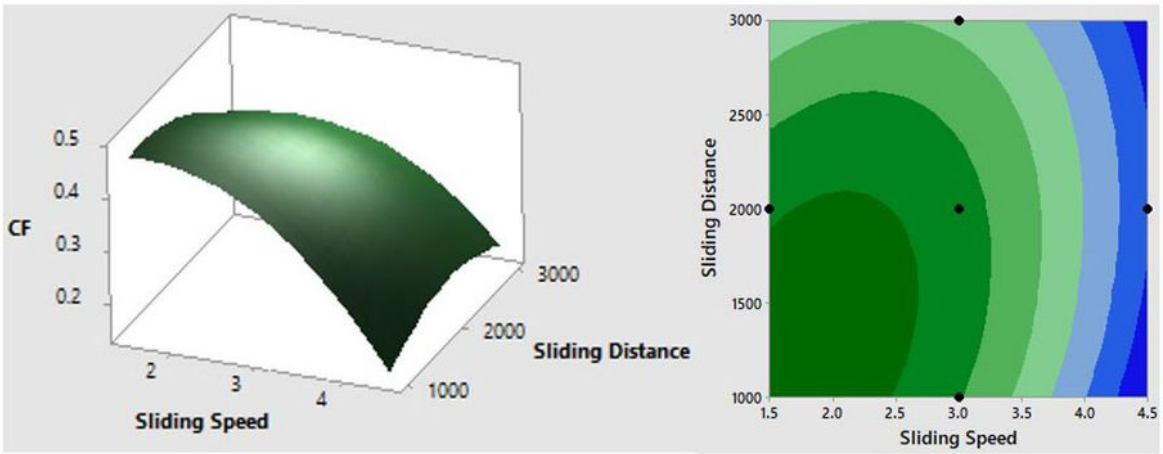

(c)

Figure 11

3D surface and contour plots for predicting the COF (a) sliding distance vs applying a load, (b) sliding speed vs applying a load, and (c) sliding speed vs sliding distance.

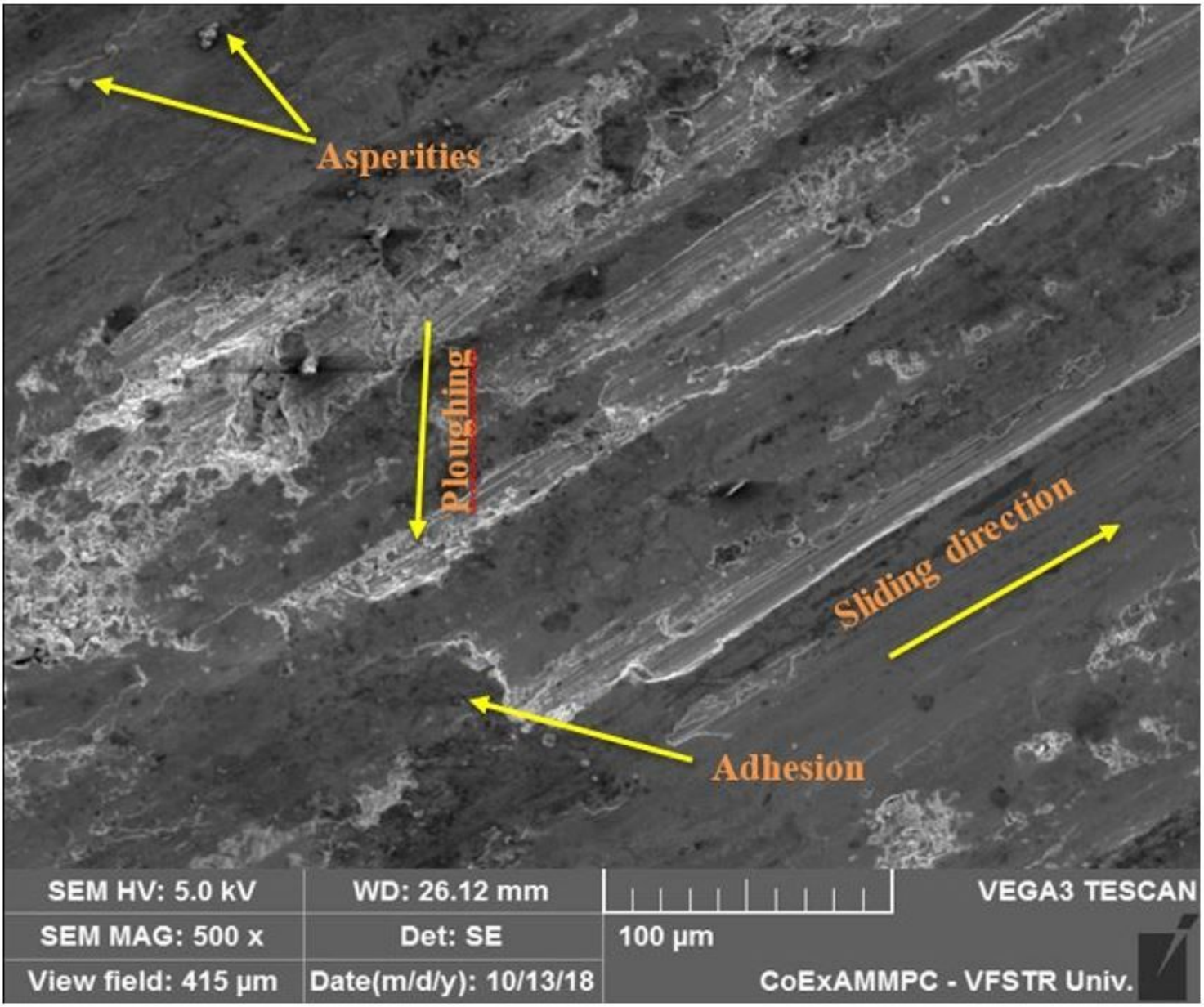

Figure 12

SEM worn surface morphology image of hybrid composite (Al 7075+ 10%FA+10% SiC).